

Two-dimensional chiral crystals in the NJL model

Stefano Carignano and Michael Buballa
*Institut für Kernphysik (Theoriezentrum),
Technische Universität Darmstadt, Germany*

(Dated: September 5, 2018)

We investigate the phase structure of the Nambu–Jona-Lasinio model at zero temperature, allowing for a two-dimensional spatial dependence of the chiral condensate. Applying the mean-field approximation, we consider various periodic structures with rectangular and hexagonal geometries, and minimize the corresponding free energy. We find that these two-dimensional chiral crystals are favored over homogeneous phases in a certain window in the region where the phase transition would take place when the analysis was restricted to homogeneous condensates. It turns out, however, that in this regime they are disfavored against a phase with a one-dimensional modulation of the chiral condensate. On the other hand, we find that square and hexagonal lattices eventually get favored at higher chemical potentials. Although stretching the limits of the model to some extent, this would support predictions from quarkyonic-matter studies.

I. INTRODUCTION

Since more than three decades, the phase diagram of quantum chromodynamics is object of intensive theoretical and experimental research [1–4]. In particular the conjecture that at low temperatures there could be a first-order chiral phase transition which ends at a critical point has received a lot of interest, since this endpoint is potentially detectable in heavy-ion experiments. However, in most studies which support this scenario, it is tacitly assumed that the order parameters of the various phases are uniform in space. On the other hand, it is not a new idea that there could be spatially modulated states in strongly interacting matter (see Ref. [5] for a recent review). Well-known examples are the proposal of an inhomogeneous ground state in nuclear matter [6], the possibility of spatial modulations in the context of pion condensation [7, 8], Skyrme crystals [9], and crystalline phases in (color-) superconductors [10–17].

For the QCD phase diagram, it has been argued some time ago that, at least in the limit of a large number of colors (N_c), the favored ground state of a dense Fermi sea of quarks should be characterized by a spatial modulation of the chiral condensate [18, 19]. More recent studies on quarkyonic matter seem to support this hypothesis [20–22].

For the physical case of three colors, Nambu–Jona-Lasinio– (NJL–) type model studies have revealed at intermediate chemical potentials and low temperatures the presence of an inhomogeneous phase where the chiral condensate assumes a spatially modulated form [23–25]. Most of the existing studies on inhomogeneous phases have restricted their analysis to simplified shapes of the chiral order parameter. The most popular example is the so-called “chiral density wave” (CDW), which basically amounts to a single plane wave [23, 24, 26]. This kind of ansatz is analogous to the so-called Fulde-Ferrel solutions proposed in (color-) superconductivity [10].

The study of a generic shape for the spatially dependent chiral condensate is a highly non-trivial task. It has recently been observed, however, that in NJL-type models the evaluation of the energy spectrum simplifies considerably when the condensate is allowed to vary only in one spatial dimension, while remaining constant along the two transverse directions [25]. In this particular case, the problem can be reduced to the 1+1-dimensional chiral Gross-Neveu model, where analytical expressions for the eigenvalue spectra are known [27–30]. This formal resemblance allows to perform an analysis of the phase diagram including these inhomogeneous phases without having to calculate numerically the energy spectrum of the model.

Within this framework it has been found that the inhomogeneous phase covers the region where a first-order chiral phase transition would occur when limiting the analysis to homogeneous phases. As a consequence the chiral critical point disappears from the phase diagram, leaving only a Lifshitz point where three second-order lines meet [25, 31]. The inclusion of vector interactions further enhances this effect and enlarges the size of the inhomogeneous phase [32].

The limitation to one-dimensional structures is of course a strong one. Especially at lower temperatures, higher dimensional modulations are expected to play an important role in (color-) superconductors [12, 14], whose dynamics bears strong formal resemblance with the one described in the NJL model. Moreover, recent quarkyonic-matter studies suggest that in the high chemical potential region, as the density of the system grows, the quark Fermi sea tends to break chiral

symmetry by forming increasingly complex crystalline (or quasi-crystalline) structures, which can be described as superpositions of several “quarkyonic chiral spirals” [21, 22].

Aside from these considerations, modulations in more than one spatial dimension are also of interest since they are unaffected by the instabilities with respect to fluctuations which prevent the formation of a true 1D crystalline structure at finite temperature [33].

The main purpose of this paper is therefore to investigate the properties of modulations of the chiral condensate occurring in more than one spatial dimension. While a complete analysis would in principle have to allow for modulations in three spatial dimensions, for computational reasons we will limit ourselves in the present work to two-dimensional crystalline shapes. The generalization to three-dimensional structures is straightforward once the formalism and the numerical procedure are set up.

II. INHOMOGENEOUS PHASES IN THE NJL MODEL

Our starting point is the two-flavor NJL Lagrangian [34],

$$\mathcal{L}_{NJL} = \bar{\psi}(i\gamma^\mu\partial_\mu - m)\psi + G((\bar{\psi}\psi)^2 + (\bar{\psi}i\gamma^5\tau_a\psi)^2), \quad (1)$$

where ψ is a quark field with two flavor and three color degrees of freedom and bare mass m , τ_a denotes the three Pauli matrices in isospin space, and G is a coupling constant.

We perform the mean-field approximation by expanding the interaction around the scalar and pseudoscalar condensates

$$\langle\bar{\psi}\psi\rangle = S(\vec{x}), \quad \langle\bar{\psi}i\gamma^5\tau_a\psi\rangle = P(\vec{x})\delta_{a3}, \quad (2)$$

which we allow to be space dependent. For later convenience, we also introduce the complex “mass” function,

$$M(\vec{x}) = m - 2G(S(\vec{x}) + iP(\vec{x})). \quad (3)$$

The mean-field Lagrangian can then be written as

$$\mathcal{L}_{\mathcal{MF}} = \bar{\psi}\gamma^0(i\partial_0 - \mathcal{H})\psi - G(S^2 + P^2), \quad (4)$$

with the effective Hamiltonian operator

$$\mathcal{H} = \gamma^0 \left[i\vec{\gamma} \cdot \vec{\partial} + m - 2G(S + i\gamma^5\tau_3P) \right]. \quad (5)$$

The mean-field thermodynamic potential per volume Ω associated with these (so far generic) spatially modulated condensates at temperature T and quark chemical potential μ contains a functional trace over the logarithm of the inverse quark propagator [35]. For its evaluation we employ imaginary time formalism and switch to momentum space. Assuming static (i.e., time-independent) condensates, we can perform the sum over Matsubara frequencies explicitly and obtain (up to a constant)

$$\Omega(T, \mu; M(\vec{x})) = \Omega_{kin}(T, \mu; M(\vec{x})) + \Omega_{cond}(M(\vec{x})), \quad (6)$$

with

$$\Omega_{cond}(M(\vec{x})) = \frac{1}{V} \int_V d^3x \frac{|M(\vec{x}) - m|^2}{4G}, \quad (7)$$

where V is the volume of the system, and

$$\Omega_{kin}(T, \mu; M(\vec{x})) = -T \sum_E \log \left(2 \cosh \left(\frac{E - \mu}{2T} \right) \right), \quad (8)$$

where the sum runs over all eigenvalues E of \mathcal{H} in color, flavor, Dirac and momentum space.

In presence of an inhomogeneous condensate, the diagonalization of \mathcal{H} is a highly non-trivial task, since quarks may exchange momenta by scattering off the condensate and, consequently, the resulting mean-field quark propagator is not diagonal in momentum space. In the following we assume a periodic shape of the chiral condensate forming a well-defined lattice structure. This implies that we can expand the spatially varying order parameter in a Fourier series,

$$M(\vec{x}) = \sum_{\vec{q}_k} M_{\vec{q}_k} e^{i\vec{q}_k \cdot \vec{x}}, \quad (9)$$

with discrete momenta \vec{q}_k forming a reciprocal lattice (RL). A generic element of \mathcal{H} in momentum space then takes the form

$$\mathcal{H}_{\vec{p}_m, \vec{p}_n} = \begin{pmatrix} -\vec{\sigma} \cdot \vec{p}_m \delta_{\vec{p}_m, \vec{p}_n} & \sum_{\vec{q}_k} M_{\vec{q}_k} \delta_{\vec{p}_m, \vec{p}_n + \vec{q}_k} \\ \sum_{\vec{q}_k} M_{\vec{q}_k}^* \delta_{\vec{p}_m, \vec{p}_n - \vec{q}_k} & \vec{\sigma} \cdot \vec{p}_m \delta_{\vec{p}_m, \vec{p}_n} \end{pmatrix}, \quad (10)$$

where $\sum_{\vec{q}_k}$ runs over the momenta of the RL, making obvious the non-diagonal momentum structure of the matrix.¹ In turn, momenta which do not differ by an element of the RL are not coupled, so that \mathcal{H} can be decomposed into a block diagonal form, where each block $\mathcal{H}(k)$ can be labelled by an element of the first Brillouin zone (BZ). This implementation of Bloch's theorem allows to decompose the eigenvalue sum in Eq. (8) into a momentum integration over the BZ times a sum over the discrete eigenvalues of each block [17].

III. TWO-DIMENSIONAL MODULATIONS

For general periodic structures, although the numerical diagonalization procedure is in principle straightforward, its practical implementation turns out to be computationally demanding. In order to simplify the problem, we therefore limit the generality of our ansatz Eq. (9) to lower-dimensional modulations. In this case, the momentum integration required for the evaluation of the thermodynamic potential may be split into the parts \vec{p}_{\parallel} along the direction of the modulation and \vec{p}_{\perp} perpendicular to it. One thus obtains, for a d -dimensional modulation,

$$\Omega_{kin} = - \int \frac{d^{3-d} p_{\perp}}{(2\pi)^{3-d}} \int_{BZ} \frac{d^d k}{(2\pi)^d} \sum_E T \log \left[2 \cosh \left(\frac{E(\vec{p}_{\perp}, \vec{k}) - \mu}{2T} \right) \right], \quad (11)$$

¹ The matrix is also non-diagonal in Dirac space, as indicated in Eq. (10). Here the chiral representation was used, and $\vec{\sigma}$ corresponds to the Pauli matrices. On the other hand, \mathcal{H} is diagonal in isospin and color.

where \vec{k} labels the BZ momenta and $E(\vec{p}_\perp, \vec{k})$ are the eigenvalues of $\mathcal{H}(\vec{k})$ for a given \vec{p}_\perp .

It has been observed that the eigenvalues in 3+1 dimensions can be evaluated by diagonalizing a dimensionally reduced \mathcal{H} (evaluated at $p_\perp = 0$) and subsequently boosting the resulting spectrum [25]. This dramatically simplifies the calculations. In particular for the case of one-dimensional modulations it allows to reuse a well-established set of analytical results without having to resort to a numerical diagonalization of the model Hamiltonian. The favored mass functions are then given by Jacobi elliptic functions, which smoothly interpolate between solitonic shapes close to the homogeneous chirally broken phase and sinusoidal shapes close to the restored phase.

Since the one-dimensional problem has already been treated extensively in previous works, the main focus of this work is on two-dimensional structures. A recent Ginzburg-Landau (GL) analysis has shown that close to the Lifshitz point one-dimensional modulations are energetically favored over higher dimensional ones in NJL-type models [36]. We therefore focus on what happens at zero temperature, where GL arguments are unable to provide reliable results. For simplicity, we restrict our calculations to the chiral limit, $m = 0$.

Without loss of generality, we assume the chiral condensate to vary in the xy -plane and to be constant in the z -direction. Unlike for the one-dimensional case, in two spatial dimensions different crystalline shapes may be realized. Therefore we consider different lattice geometries and assume the mass functions to have simple symmetric shapes consistent with these structures.

The first case is a square lattice with a unit cell spanned by two perpendicular vectors of length a in x and y direction. The corresponding elements of the RL are then given by $\vec{q}_{m,n} = Q(m\vec{e}_x + n\vec{e}_y)$ with $Q = 2\pi/a$ and integers m and n . While the general mass function consistent with this lattice structure would be given by Eq. (9) with arbitrary Fourier coefficients $M_{m,n}$, we restrict ourselves to a simple ansatz for a real symmetric mass function with a small number of nonvanishing Fourier coefficients. Specifically we choose $M_{1,1} = M_{1,-1} = M_{-1,1} = M_{-1,-1} = M/4$ and $M_{m,n} = 0$ in all other cases.² This yields

$$M(x, y) = M \cos(Qx) \cos(Qy), \quad (12)$$

which has an egg-carton-like shape (see Fig. 1, left) and is symmetric under discrete rotations by $\pi/2$.

The second case we consider is a mass function with hexagonal symmetry. Here we start from a unit cell spanned by two vectors of length a , enclosing an angle of $\pi/3$. Choosing the first one to be aligned with the x -axis, the elements of the RL are given by $\vec{q}_{m,n} = Q(m\vec{e}_x + \frac{2n-m}{\sqrt{3}}\vec{e}_y)$, with integers m and n , and $Q = 2\pi/a$ as before. For the mass function we choose $M_{m,n} = M/6$ on the corners of a regular hexagon, $(m, n) \in \{(1, 0), (-1, 0), (0, 1), (0, -1), (1, 1), (-1, -1)\}$, and $M_{m,n} = 0$ in all other cases. This yields

$$M(x, y) = \frac{M}{3} \left[2 \cos(Qx) \cos\left(\frac{1}{\sqrt{3}}Qy\right) + \cos\left(\frac{2}{\sqrt{3}}Qy\right) \right], \quad (13)$$

² An alternative choice would be $M_{1,0} = M_{-1,0} = M_{0,1} = M_{0,-1} = M/4$ and $M_{m,n} = 0$ in all other cases, which yields $M(x, y) = \frac{M}{2}(\cos(Qx) + \cos(Qy))$. However, this is equivalent to Eq. (12) in a frame rotated by $\pi/4$ and Q replaced by $Q/\sqrt{2}$.

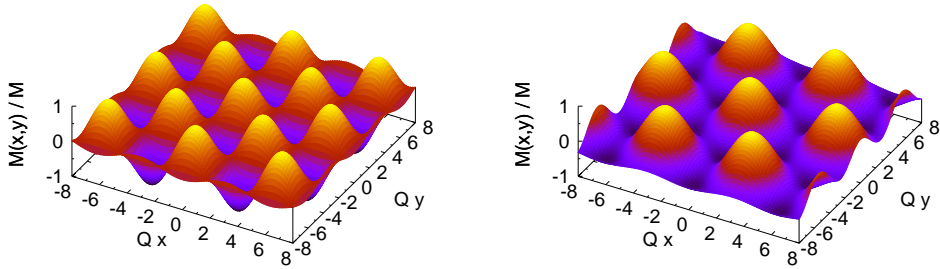


FIG. 1. Mass functions $M(x, y)$ with two-dimensional modulations in coordinate space. Left: “egg-carton” modulation on a square lattice, Eq. (12). Right: hexagonal modulation, Eq. (13).

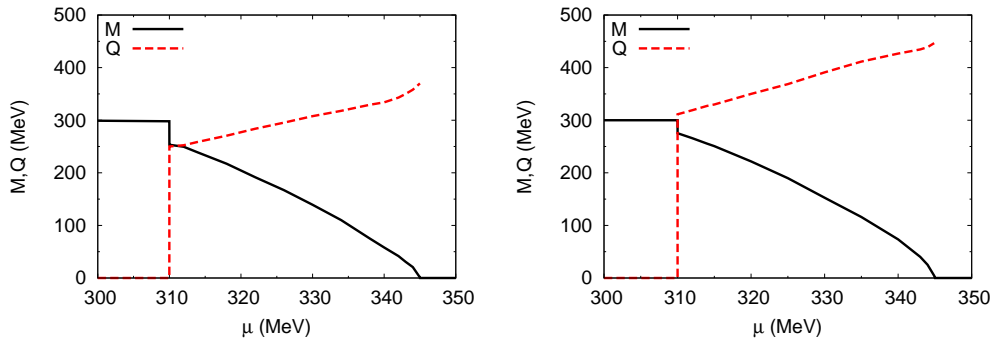


FIG. 2. Amplitude M and wave number Q at $T = 0$ as functions of the chemical potential μ after minimization of the thermodynamic potential for given shapes of the mass function. Left: “egg-carton” modulation on a square lattice, Eq. (12). Right: hexagonal ansatz, Eq. (13).

which is symmetric under discrete rotations by $\pi/3$ (see Fig. 1, right). Note that the normalization of the amplitude was chosen to match the homogeneous case $M(x, y) = M$ when Q goes to zero.

After inserting these shapes into Eq. (10), the Hamiltonian is diagonalized numerically in Dirac and momentum space, and the thermodynamic potential is minimized with respect the variational parameters M and Q , characterizing amplitude and period of the modulations. For the numerical calculations, we have to specify a procedure to regularize the integrals and eigenvalue sum in Eq. (11). Following Refs. [25, 32, 37], we use a Pauli-Villars scheme with three regulators. For the results in this section, we fit our model parameters (the regulator Λ and the coupling constant G) to reproduce the pion decay constant in the chiral limit, $f_\pi = 88$ MeV, and a vacuum constituent quark mass of $M_{vac} = 300$ MeV [25].

The results of the numerical minimization for the square and hexagonal shapes, Eqs. (12) and (13) respectively, are presented in Fig. 2. For both modulations, we find a sharp onset of the crystalline phase around $\mu \approx 310$ MeV and a smooth approach to the restored phase, which is reached at $\mu \approx 345$ MeV via a second-order phase transition as the amplitude of the chiral condensate melts to zero. For the transition to the homogeneous chirally broken phase, the situation

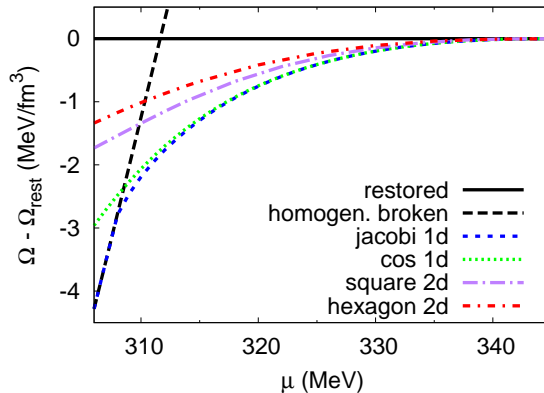


FIG. 3. Thermodynamic potential relative to the restored phase for different modulations of the chiral condensate at $T = 0$. The homogeneous broken and restored solutions are disfavored compared to the crystalline phases in a window between $\mu \approx 308$ and $\mu \approx 345$ MeV. The lowest free energy is found for the one-dimensional Jacobi elliptic function. In particular at the onset of the inhomogeneous phase it is favored over a one-dimensional cosine, while with increasing μ the two shapes quickly become almost degenerate. The two-dimensional square ansatz, Eq. (12), is always disfavored against the one-dimensional modulations, and the hexagonal crystal, Eq. (13), leads to an even smaller gain in free energy.

is therefore different from the case of one-dimensional solitonic solutions [25] and might be due to our limited ansatz with a finite number of Fourier components. We also note that the results for the amplitude M are comparable for both shapes in the inhomogeneous window.

The results presented in Fig. 2 have been obtained by enforcing in each case a fixed shape of the chiral modulation. Under this restriction we found a window where the different two-dimensional solutions are energetically favored over the homogeneous solutions. This is basically the same region where one-dimensional modulations are also found to be favored over homogeneous solutions. In fact, as shown in Ref. [31] using GL arguments, the critical chemical potential for the transition from the inhomogeneous to the chirally restored phase is independent of the shape of the spatial modulation, as long as the phase transition is second order.

The next obvious step is to compare the free energies of these solutions with each other, in order to find out which of them corresponds to the most stable solution. The results of our comparison are shown in Fig. 3. One can clearly see that the one-dimensional Jacobi elliptic functions lead to the biggest gain in free energy compared to all the other cases considered. In particular, the two-dimensional structures turn out to be energetically disfavored with respect to one-dimensional real modulations throughout the whole inhomogeneous window.

In this context it is instructive to introduce a rectangular structure, which interpolates continuously between a square lattice and a one-dimensional periodic modulation. Specifically, we can generalize the “egg-carton” ansatz Eq. (12) to

$$M(x, y) = M \cos(Q_x x) \cos(Q_y y), \quad (14)$$

which reduces to a single cosine varying in one spatial dimension when one of the two wave numbers

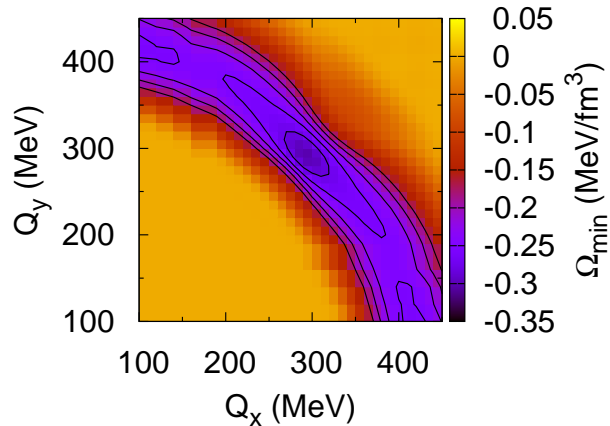


FIG. 4. Value of the thermodynamic potential at $T = 0$ and $\mu = 325$ MeV for a rectangular lattice, Eq. (14), as a function of Q_x and Q_y . At each point, Ω was minimized with respect to M .

goes to zero.

Starting from this ansatz, we minimize the thermodynamic potential with respect to the amplitude M for fixed wave numbers Q_x and Q_y , and then study the result as a function of Q_x and Q_y . Since we know already that the square-lattice solution along the line $Q_x = Q_y$ is disfavored against the one-dimensional cosine, we are mainly interested in the question whether the former corresponds to a local minimum or to a saddle point in the $Q_x - Q_y$ plane.

Our result for $\mu = 325$ MeV is presented in Fig. 4, showing that the solution at $Q_x = Q_y$ is a local minimum. One can also see that in the vicinity of the minimum the potential remains rather flat along the direction perpendicular to the line $Q_x = Q_y$. Going along this valley, we find two saddle points at $(Q_x, Q_y) \approx (175 \text{ MeV}, 400 \text{ MeV})$ and $(400 \text{ MeV}, 175 \text{ MeV})$. Unfortunately, the computing time rises strongly with decreasing wave numbers, so that we could not continue this analysis to values of Q_x or Q_y lower than 100 MeV. However, it is not hard to imagine how beyond the saddle points the valley approaches the absolute minima at vanishing Q_x or Q_y , corresponding to a one-dimensional cosine.

One may ask whether our observation that the two-dimensional crystalline structures are disfavored against the one-dimensional ones is caused by the restricted ansatz for the mass functions. Taking into account more Fourier modes would lead to additional variational parameters and could thus lower the free energy. It is however unlikely that this would change our results considerably. As seen in Fig. 3 the difference in free energy between the Jacobi elliptic function and the one-dimensional cosine is negligible in a large chemical-potential range and always much smaller than the difference to the two-dimensional solutions. We therefore expect that the corrections to the considered two-dimensional shapes are small as well.

In order to test this, we extend the simple “egg carton” ansatz (Eq.12) into

$$M(x, y) = \sum_{n=1}^3 M_n \cos(nQx) \cos(nQy) \quad (15)$$

The minimization of the thermodynamic potential with respect to the variational parameters (M_1, M_2, M_3, Q) leads, within numerical errors, to $M_2 = M_3 = 0$ throughout the whole inhomogeneous window. Although numerical errors are more significant than for the one-dimensional case, it is safe to say that the inclusion of those higher harmonics considered above does not lead to an appreciable gain in free energy.

IV. HIGHER CHEMICAL POTENTIALS

In recent quarkyonic-matter studies it was found that increasing the chemical potential leads to two-dimensional structures with growing geometrical complexity [22]. While no definite scale was given, this could be a hint that the chemical potentials we have considered so far are too low for two-dimensional crystals to be favored. This motivates us to extend our investigations to higher values of μ .

In fact, while so far we have concentrated on the inhomogeneous “island” close to the would-be first-order phase boundary for homogeneous phases, we have recently found that in the NJL model a second inhomogeneous region (“continent”) appears at higher μ and seemingly persists to arbitrarily high chemical potentials [37]. Of course, we have to keep in mind that the NJL model is a low-energy effective model with a limited range of validity. In particular, since the continent appears in a region where the chemical potential is of the order of the regulator masses, we have to be cautious not to overinterpret the results. However, as thoroughly discussed in Ref. [37], although the inhomogeneous continent is sensitive to regularization effects, it is not obviously created by them. Indeed, there is no a priori reason to exclude the possibility of an inhomogeneous chiral symmetry breaking phase at high chemical potentials. For instance, inhomogeneous phases extending to arbitrarily high chemical potentials have been predicted for the Gross-Neveu model and its chiral counterpart [27], for quarkyonic matter [22] and for QCD in the large- N_c limit [18]. Here we do not want to enter this discussion, but simply take the inhomogeneous continent as a “model laboratory” to study the competition of one- and two-dimensional chiral crystals as a function of μ .

Figure 5 shows the free energies associated with the one-dimensional solitonic solutions and the two-dimensional “egg carton” close to the phase transition marking the onset of the inhomogeneous continent (the second-order nature of the transition from the restored phase is visible in the behaviour of both free energies). From this comparison, it is possible to see that in this region, two-dimensional solutions become favored over one-dimensional ones. Since with the current parameter set the continent is not connected to the the inhomogeneous island, it is not clear at which point higher-dimensional structures become favored. In order to achieve a better understanding of the problem, in the following we therefore employ a slightly modified parameter set with a vacuum constituent quark mass of 330 MeV. This does not modify any qualitative behaviour of the

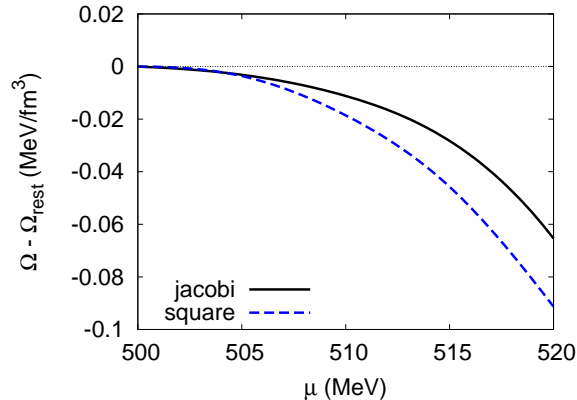


FIG. 5. Free energies associated with the one-dimensional solitonic solutions (black solid line) and the two-dimensional “egg-carton” (blue dashed line) at the onset of the second inhomogeneous phase, occurring around $\mu = 500$ MeV. Results are calculated for $T = 0$ with a parameter set fitted to give a vacuum constituent quark mass of $M_{vac} = 300$ MeV, and are normalized with respect to the free energy of the restored phase.

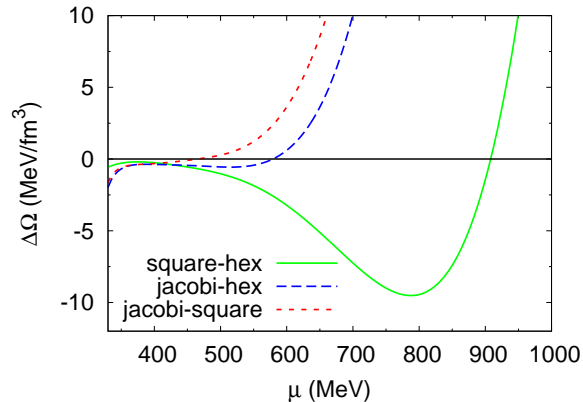


FIG. 6. Free-energy differences between inhomogeneous phases with different modulations, evaluated at $T = 0$ and with a parameter set fitted to give a vacuum constituent quark mass of $M_{vac} = 330$ MeV.

model but has the advantage that the inhomogeneous island merges with the continent, so that the comparison of the inhomogeneous phases can be performed on a continuous interval, without being interrupted by the restored phase.

In Fig. 6 the differences between the free energies of three inhomogeneous phases with different modulations are displayed as functions of μ . As we have seen before, at low chemical potentials the two-dimensional crystals are disfavored against the one-dimensional Jacobi elliptic function. Above $\mu \approx 450$ MeV, however, the two-dimensional square lattice leads to a lower free energy. At $\mu \approx 600$ MeV, also the hexagon surpasses the one-dimensional modulation and finally becomes the most favored shape at $\mu \approx 900$ MeV. Thus, while being aware that the model cannot be trusted blindly in this high density region, it is nevertheless remarkable that we recover the same sequence of crystalline phases as described in Ref. [22].

V. DISCUSSION AND OUTLOOK

In this paper we presented the results of our numerical study of two-dimensional chiral crystalline structures in the NJL model at zero temperature. At intermediate chemical potentials, in the region where the chiral phase transition would take place if the analysis was restricted to homogeneous condensates, we find that two-dimensional modulations are disfavored against one-dimensional ones, indicating that their greater kinetic energy cost is not sufficiently compensated by a larger gain in condensation energy. We also find that a hexagonal structure is even less favored than a square lattice in this regime.

From these observations, it seems unlikely that a phase where the chiral condensate is modulated along three spatial dimensions could become thermodynamically favored, due to its even higher kinetic-energy cost. Moreover, since a GL analysis has revealed that also close to the Lifshitz point phases with higher-dimensional modulations are disfavored against one-dimensional ones [36], we do not expect that higher-dimensional structures appear at finite temperature, at least in mean-field approximation. A numerical analysis to confirm these expectations would of course be desirable.

The situation gets successively reversed when we increase the chemical potential. At a certain value, we find that the structure of the ground state changes from having one-dimensional modulations to a two-dimensional square lattice and, at even higher μ , to an hexagonal shape. Although the results must not be trusted blindly in this high-density regime, which lies at the edge of the expected range of validity of the model, we find it nevertheless noteworthy that we reproduce qualitatively the behavior recently proposed for quarkyonic matter [22]³. It is also interesting that a similar sequence of phases was predicted for a 2D superconductor in a magnetic field [12]. On the other hand, the chemical potentials where the two-dimensional structures appear in our model belong to the realm of color superconductivity. Therefore it would be important to include the effects of diquark pairing as well.

ACKNOWLEDGMENTS

We thank Y. Hidaka, T. Kojo, L. McLerran, D. Nickel and J. Wambach for illuminating discussions. This work was partially supported by the Helmholtz Alliance EMMI, the Helmholtz International Center for FAIR, and by the Helmholtz Research School for Quark Matter Studies H-QM.

-
- [1] M. A. Halasz, A. D. Jackson, R. E. Shrock, M. A. Stephanov, and J. J. M. Verbaarschot, *Phys. Rev. D* 58, 096007 (1998).
 - [2] M. A. Stephanov, *Prog. Theor. Phys. Suppl.* 153, 139 (2004).
 - [3] P. Braun-Munzinger and J. Wambach, *Rev. Mod. Phys.* 81, 1031 (2009).

³ Quasicrystalline structures with discrete rotational symmetries higher than six, which have also been discussed in Ref. [22], are much more difficult to implement in our model since we heavily rely on the translational periodicity to perform our numerical calculations. These structures are anyway expected to appear only at even higher chemical potentials.

- [4] K. Fukushima and T. Hatsuda, Rept. Prog. Phys. 74, 014001 (2011).
- [5] W. Broniowski, Acta Phys. Pol. B Proc. Suppl. 5/3, 631 (2012), arXiv:1110.4063 [hep-ph].
- [6] A. W. Overhauser, Phys. Rev. 128, 1437 (1962).
- [7] F. Dautry and E. Nyman, Nucl. Phys. A 319, 323 (1979).
- [8] W. Broniowski, A. Kotlorz, and M. Kutschera, Acta Phys. Pol. B 22, 145 (1991).
- [9] A. S. Goldhaber and N. S. Manton, Phys. Lett. B 198, 231 (1987).
- [10] P. Fulde and R. A. Ferrell, Phys. Rev. 135, A550 (1964).
- [11] A. I. Larkin and Y. N. Ovchinnikov, Zh. Eksp. Teor. Fiz. 47, 1136 (1964); Sov. Phys. JETP 20 762 (1965).
- [12] Y. Matsuda and H. Shimahara, J. Phys. Soc. Jpn. 76, 051005 (2007).
- [13] M. G. Alford, J. A. Bowers, and K. Rajagopal, Phys. Rev. D 63, 074016 (2001).
- [14] J. A. Bowers and K. Rajagopal, Phys. Rev. D 66, 065002 (2002).
- [15] R. Casalbuoni, M. Ciminale, M. Mannarelli, G. Nardulli, M. Ruggieri and R. Gatto, Phys. Rev. D 70, 054004 (2004).
- [16] K. Rajagopal and R. Sharma, Phys. Rev. D 74, 094019 (2006).
- [17] D. Nickel and M. Buballa, Phys. Rev. D 79, 054009 (2009).
- [18] D. V. Deryagin, D. Y. Grigoriev, and V. A. Rubakov, Int. J. Mod. Phys. A 7, 659 (1992).
- [19] E. Shuster and D. T. Son, Nucl. Phys. B 573, 434 (2000).
- [20] T. Kojo, Y. Hidaka, L. McLerran, and R. D. Pisarski, Nucl. Phys. A 843, 37 (2010).
- [21] T. Kojo, R. D. Pisarski, and A. M. Tselik, Phys. Rev. D 82, 074015 (2010).
- [22] T. Kojo, Y. Hidaka, K. Fukushima, L. McLerran, and R. D. Pisarski, Nucl. Phys. A 875, 94 (2012).
- [23] M. Sadzikowski and W. Broniowski, Phys. Lett. B 488, 63 (2000).
- [24] E. Nakano and T. Tatsumi, Phys. Rev. D 71, 114006 (2005).
- [25] D. Nickel, Phys. Rev. D 80, 074025 (2009).
- [26] I. Frolov, V. Zhukovsky, and K. Klimenko, Phys. Rev. D 82, 076002 (2010).
- [27] O. Schnetz, M. Thies, and K. Urlichs, Annals Phys. 314, 425 (2004).
- [28] O. Schnetz, M. Thies, and K. Urlichs, Annals Phys. 321, 2604 (2006).
- [29] M. Thies, J. Phys. A 39, 12707 (2006).
- [30] G. Basar, G. V. Dunne, and M. Thies, Phys. Rev. D 79, 105012 (2009).
- [31] D. Nickel, Phys. Rev. Lett. 103, 072301 (2009).
- [32] S. Carignano, D. Nickel, and M. Buballa, Phys. Rev. D 82, 054009 (2010).
- [33] G. Baym, B. Friman, and G. Grinstein, Nucl. Phys. B 210, 193 (1982).
- [34] Y. Nambu and G. Jona-Lasinio, Phys. Rev. 124, 246 (1961).
- [35] J. Kapusta and C. Gale, Finite-Temperature Field Theory - Principles and Applications, second ed., Cambridge University Press (2006).
- [36] H. Abuki, D. Ishibashi, and K. Suzuki, Phys. Rev. D 85 074002 (2012).
- [37] S. Carignano and M. Buballa, Acta Phys. Pol. B Proc. Suppl. 5/3, 641 (2012), arXiv:1111.4400 [hep-ph].